Proceedings of the Canadian Society for Mechanical Engineering International Congress
32nd Annual Conference of the Computational Fluid Dynamics Society of Canada
Canadian Society of Rheology Symposium
CSME/CFDSC/CSR 2025
May 25–28, 2025, Montréal, Québec, Canada

ID 505

Large-Eddy Simulation of Turbulent Premixed Hydrogen-Air Bunsen Flames Using PCM-FPI Combustion Model

Stefano Binato[1,2,*] and Clinton P. T. Groth[1]

[1]Institute for Aerospace Studies, University of Toronto, 4925 Dufferin Street, Toronto, Ontario, Canada, M3H 5T6
[2]Institute for Fluid Dynamics, Eidgenössische Technische Hochschule Zurich, Sonnegstrasse 3, 8092 Zurich, Switzerland
[*]sbinato@ethz.ch

March 29, 2025

***Abstract*—Hydrocarbon fueled combustion offers an effective pathway to reducing harmful green-house gas emissions associated with carbon dioxide. Nevertheless, diffusion effects are known to be important in turbulent premixed flames involving hydrogen as a fuel, and the ability to predict these effects accurately will be fundamental to arriving at effective numerical combustion models needed for hydrogen flames. For perfectly premixed flames, the further away from the preferential diffusion neutral condition with an equivalence ratio, ϕ, of $\phi = 1.8$, the strongerits effects. In addition, diffusive-thermal effects also manifest their contributions, for which the neutrally stable condition is located for values of $\phi = 0.8$. In this study, Large-Eddy Simulation (LES) of turbulent premixed hydrogen-air flames is considered using the so-called Presumed Conditional Moment - Flame Prolongation of Intrinsic low-dimensional manifold (PCM-FPI) combustion model for a number of flames around the neutral condition towards both the lean and rich limits. Premixed Bunsen-type flames with equivalent ratios in the range $0.8 \leq \phi \leq 3.57$ and for Reynolds numbers of $\mathrm{Re} = 20,000$ and 40,000 are examined and the LES predictions are compared to available experimental data from previous studies. The comparisons illustrate the mutual influence of turbulence and diffusion phenomena on the turbulent flame structure, burning rate, and flame height. In the lean limit with unstable diffusion conditions, overprediction of flame height and underprediction of turbulent burning rate are observed. Furthermore, the contribution of the instabilities on flame wrinkling decreases with turbulence intensity leading to reductions in these predicted errors. The opposite is true in the rich limit.

***Keywords*—hydrogen combustion; premixed turbulent flames; large-eddy simulation (LES); preferential diffusion; diffusive-thermal effects; Bunsen burner.**

I. Introduction and Motivation

Hydrocarbon combustion related environmental issues associated with the production of carbon dioxide (CO_2) and other emissions are no longer new to the scientific community. It is now well established that there is direct correlation between green-house gases emissions and the rise of the average global temperature (see "Our World in Data", "International Energy Agency" (IEA), or [1], [2]). The milestones for reduction in CO_2 emissions currently sought world-wide (see "Paris Agreement"), can be achieved partially by blending conventional hydrocarbon fuels with hydrogen, or in the best case, substituting current hydrocarbon fueled combustion energy conversion systems with those fueled by pure hydrogen. However, as hydrogen combustion can be generally characterized by relatively thin flames, higher burning rates, and the enhanced molecular diffusivity of hydrogen relative to other gaseous molecules, it is therefore not possible to project directly knowledge from hydrocarbon combustion behaviour to that for hydrogen. New knowledge and understanding is required specific to the combustion of hydrogen. Accordingly, as reported by the IEA, the level of funding and research to support efforts to convert to hydrogen-based combustion has progressively increased in the last 5-10 years. Considerable research efforts are now being made in a variety of areas, from the combustion of hydrogen via a chemical energy carrier such as ammonia to its direct application in internal combustion as well as gas turbine engines. These research efforts involve both experimental studies and numerical modelling of hydrogen combustion processes.

A. *Previous Studies of Hydrogen Combustion*

While the literature on hydrogen combustion is far too extensive to review here, in terms of previous experimental studies, there is an overall lack of experimental studies on turbulent premixed hydrogen combustion, both for understanding of the combustion issues associated with flame speed, flashback, lift-off, and blow-off and for the validation of numerical modelling strategies. This is due in part to concerns with safety, to issues associated with the complexity of premixed burner designs so as to avoid flash back, and also partly to the availability and costs of equipment required for performing and collecting the required experimental data. Böhm *et al.* [3] provide a review of some of the relevant experimental techniques both for non-premixed [4]–[7] and premixed hydrogen flames. The latter is considered to be of more engineering relevance for gas turbine engines, at least for power generation, because this allows control of the combustion via mixture composition independent of the mixing process. Previous experimental studies on hydrogen that could be used for validation purposes include studies of outwardly propagating flames [8], [9], counter-flow jet flames [10], Bunsen flames [11]–[15], as well as swirl stabilized flames [16]–[18].

As an alternative to experimental studies, Direct Numerical Simulations (DNS) methods [19] can be used. Nevertheless, today DNS are still extremely computationally expensive. Compared to DNS, Large-Eddy Simulation (LES) methods are a more economical solution to capture engineering relevant phenomena and abate prohibitive computational costs. Nevertheless, for turbulent reactive flows, additional modelling of the influences of turbulence-chemistry interactions that occur at the smallest unresolved scales is required for effective LES strategies and currently most of the standard LES models are not able to capture the complex preferential diffusion phenomena, which are particularly pronounced in hydrogen flames. In terms of head-to-head comparisons of LES predictions to experiment for premixed flames, the authors are aware of only a few previous studies that consider preferential diffusion effects: Kai *et al.* [20] recently compare predictions of a LES flamelet model to the experimental data of Shoji *et al.* [21]) for lean premixed hydrogen low-swirl flames and more recently the studies [22], [23] have demonstrated that the performance of LES for swirling premixed flames in micro-mix combustors is improving; however, preferential diffusion phenomena, which have been established for more than thirty-five years [14], [15] and widely discussed since then, are still not well captured.

B. Diffusion Processes in H_2 Combustion

In the previous experimental studies by Wu *et al.* [14], [15], it was shown how preferential diffusion impacts the combustion characteristics of pure turbulent premixed hydrogen flames. Using a simple Bunsen burner setup, Wu *et al* show through schlieren, Rayleigh scattering, and laser velocimetry measurements that, starting from a neutrally-stable equivalence ratio (found to be around $\phi = 1.8$) and for comparable levels of turbulence as measured by $\bar{u}'/S_L$, where $\bar{u}'$ is the root-mean-square of the turbulent fluctuations and S_L is the laminar flame speed, preferential diffusion has a stabilizing effect for rich fuel/air mixtures and destabilizing effects for lean mixtures. To understand this behaviour, it is enough to think of the flame as a sink and to consider the two-dimensional case, for which the burnt product gases start to penetrating the fuel-air mixture creating a "C"-shaped zone in a weakly wrinkled planar flame. The "C"-shaped region separates the fresh mixture on the left, and the burnt gases on the right. For the lean case, because the flame consumes the reactants, the hydrogen molecules that diffuse faster than the the other larger gaseous species from the surrounding regions reach more rapidly the flame zone and locally generate an increase in ϕ, that for a lean mixture is associated with a higher laminar burning velocity or speed. This enhances the wrinkling, and therefore the flame area, with a consequent increase in the local turbulent burning velocity. The same happens for the stable region, where the hydrogen concentrates increasing locally the equivalence ratio, but in this case leads to reduced flame wrinkling. The schlieren images in [14] and Fig. 2 clearly show the differences in the observed premixed flame behaviour in the unstable ($\phi < 1.8$), neutral ($\phi = 1.8$), and stable ($\phi > 1.8$) preferential diffusion regimes. Note that this effect occurs as described for fuels with Lewis number $\mathrm{Le} = \alpha_D / D < 1$, for which the mass diffusivity, D, is significantly larger than the thermal diffusivity, α_D. On the other hand, for the range of values of the Lewis number, $\mathrm{Le} < 1$, diffusive-thermal effects caused by the positive stretch of the turbulent Bunsen-burner flames combines with preferential diffusion to increase the burning velocity [24]. However, for diffusive-thermal effects, the neutral region has been demonstrated to be around $\phi \approx 0.8$. This generally separates the unstable region associated with leaner mixture and the stable region of richer mixtures.

II. Scope of the Present Study

The present study considers the application of LES using the standard flamelet-type subfilter-scale (SFS) combustion model, the so-called Presumed Conditional Moment - Flame Prolongation of Intrinsic low-dimensional manifold (PCM-FPI) combustion model of Gicquel *et al.* [25], Domingo *et al.* [26], and Galpin *et al.* [27] as previously implemented and successfully applied to turbulent premixed flames of hydrocarbon fuels by Hernández-Pérez *et al.* [28]–[30] and Shahbazian *et al.* [31], to turbulent premixed Bunsen-type hydrogen flames previously examined in the experimental studies of Wu *et al.* [14], [15] with equivalent ratios in the range $0.8 \leq \phi \leq 3.57$ and for the jet-stream Reynolds numbers of $\mathrm{Re} = 20,000$ and 40,000. The PCM-FPI LES predictions are systematically compared to the available experimental data from the previous studies with the goal of carefully assessing and quantifying the discrepancies caused by diffusional effects in the hydrogen flames as a function of the fuel equivalence ratio, ϕ. The comparisons will illustrate the mutual influence of turbulence and preferential and thermal diffusive effects on the flame structure, burning rate, and flame height and highlight the issues associated with flamelet-type combustion models when applied to turbulent premixed hydrogen flames.

III. Turbulent Premixed Hydrogen-Air Flames

A. Premixed Bunsen Burner

The Bunsen flame experimental setup considered by Wu *et al.* [14], [15] is depicted in Fig. 1 and the matrix of turbulent premixed flames examined as part of their experimental effort is summarized in Table I. The burner is characterized by a central jet the exit velocity of which was adapted to match the target Reynolds number and a hot co-flow pilot of burnt gases that was used to ensure the combustion occurred under adiabatic conditions. The burner fuel line diameter was $d=11$ mm and the external radius of the burner was $R=29$ mm. Originally, Wu *et al.* intended to conduct their experiments with a co-flow that matched exactly the equivalence ratio of the central premixed jet, but it was noticed that the co-flow pilot did not influence the resulting premixed flame as the mixing line between the co-flow and burnt gases proved to be sufficiently far from the flame as shown in Fig. 1. This was also verified by the present LES simulations. Therefore, the co-flow pilot had a fixed equivalence ratio of $\phi=0.3$. However, for the sake of simplicity, the co-flow in the LES was assumed to match the properties of the burnt gases of the central flame, thereby ensuring the adiabaticity of the simulated flames. The fresh gas temperature in the experiments was $T_u = 300$ K and all of the experiments were conducted under atmospheric conditions with $p=1$ atm.

B. LES Setup

The preceding experimental setup was reproduced in the LES here using a cylindrical-type body-fitted mesh consisting of 2 million computational cells using a computational domain with height, H, that was adapted to the experimental flame height, L_c, such that that the domain outlet did not affect the flame tip solutions: $1.5L_c < H < 3L_c$. The isotropic inflow turbulence for the premixed jet was pre-generated using a Haworth-Poinsot spectrum [32] and the method of Rogallo [33]. The turbulence intensity was estimated by Wu *et al.* to be $\overline{u}'/\overline{u} \approx 0.1$ and, assuming isotropic turbulence, the total turbulence kinetic energy (TKE), $k = (3/2)\overline{u}'^2$, was taken to match the experimental values. In the LES solution procedure, the Favre-filtered form of the Navier-Stokes equations for a compressible reactive mixture are solved using a second-order finite-volume scheme applied to hexahedral multi-block computational mesh. For the LES modelling, the unresolved SFS stresses, σ_{ij}, are explicitly treated using either the standard Smagorinsky model or a one-equations SFS stress model based on the solution of a SFS TKE equation [30]. Additionally, the SFS enthalpy and species fluxes are evaluated using standard gradient approximations. In the associated finite-volume solution method, the inviscid numerical fluxes are evaluated using the Riemann-solver based flux function of Roe [34] in combination with limited, piecewise, linear, least-squares solution reconstruction and the resulting semi-discrete form of the governing equations are integrated forward in time using a standard second-order Runge-Kutta time marching scheme. The reader is referred to the thesis of Hernández-Pérez [30] for a summary of the LES modelling adopted herein and a detailed description of the finite-volume solution procedure.

C. PCM-FPI

A complication of LES for turbulent premixed combustion is that the chemical reactions occur within thin or narrow flame fronts at extremely small scales that are generally not resolved on typical LES grids. Thus, the role of SFS models for turbulence-chemistry interactions in LES of premixed combustion is of significant importance. In the LES approach considered herein, the filtered reaction rates, $\tilde{\dot{\omega}}_\alpha$, for a given species α are modelled using the PCM-FPI combustion model. This combustion model [25]–[27] is a flamelet-based chemistry tabulation model that makes use of pre-tabulated steady, one-dimensional, premixed flame solutions to represent the chemistry in three-dimensional turbulent flames. In particular, in the Flame Prolongation of Intrinsic low-dimensional manifold or FPI tabulated approach [25] relevant chemical quantities such as species mass fractions, Y_α, and species reaction rates, $\dot{\omega}_\alpha$, that are evaluated based on the steady-state, laminar, premixed flamelet solutions for a given equivalence ratio, ϕ_0, or given mixture fraction, Z_0. At a given position within the one-dimensional flame, x, the laminar solutions are mapped in terms of a progress of reaction variable, Y_c. The progress of reaction is generally a function of the mass fraction of relevant species and, accordingly, any quantity, φ, within the flame can be evaluated as

$$\varphi^{FPI}(Z_0, c) = \varphi^{FPI}(\phi_0, Y_c) = \varphi(\phi_0, x)\,, \qquad (1)$$

where $c = Y_c/Y_c^{EQ}(Z_0)$ is the normalized progress variable. The quantity, Y_c, should be selected such there is a unique one-to-one value of the various tabulated quantities, φ^{FPI}, as function of Y_c. For this study, as in other previous investigations involving premixed hydrogen combustion, $Y_c = Y_{H_2O}$ is used.

For treating the turbulence-chemistry interaction, the PCM-FPI method adopts a statistical approach that makes use of an assumed PDF, $\tilde{P}(c)$, for the SFS fluctuations in the progress variable, c, when evaluating the SFS reaction rates $\dot{\omega}_\alpha(T, Y_{\alpha_1}, ..., Y_{\alpha_N})$. Using the FPI tabulation for a given premixed laminar flame with equivalence ratio, ϕ_0, or mixture fraction, Z_0, the resulting filtered quantities, $\tilde{\varphi}$, including filter reaction rates, are determined and tabulated using

$$\tilde{\varphi} = \int_0^1 \varphi^{FPI}(Z_0, c)\tilde{P}(c)\,\mathrm{d}c\,, \qquad (2)$$

where $\tilde{P}(c)$ is assumed to have a β-distribution. The parameters defining the β-distribution are determined based on predicted values of the filtered progress variable, $\tilde{Y}_c$, and its variance, $Y_{cv} = \widetilde{Y_c Y_c} - \tilde{Y}_c\tilde{Y}_c$.

TABLE. I
TURBULENT BUNSEN FLAME TEST CONDITIONS

ϕ	$\overline{u}^{\square}_{\text{avg}}$ (m/s)	$\overline{u}'^{\star}_{\text{avg}}/S_L$	$L^{\circ}_c/d^{\blacktriangledown}$
$Re = 20000$, $Re_t^{\triangle} = 800$			
0.80	36.0	1.6	3.7
1.00	37.9	1.4	3.2
1.80	45.0	1.3	3.3
3.57	58.3	2.5	7.7
$Re = 40000$, $Re_t = 1800$			
0.80	72.0	3.3	5.4
1.00	75.8	2.8	4.8
1.80	90.0	2.6	5.3
3.57	116.4	5.0	11.7

$^{\square}$Mean jet exit velocity; *rms fluctuation; $^{\blacktriangledown}$Fuel line diameter;
$^{\circ}$Flame height defined on combustion progress variable $\overline{c} = 0.5$;
$^{\triangle}$Turbulent Reynolds number: $Re_t = \overline{u}'\,0.4d/\nu_0$, ν_0 kin. viscosity.

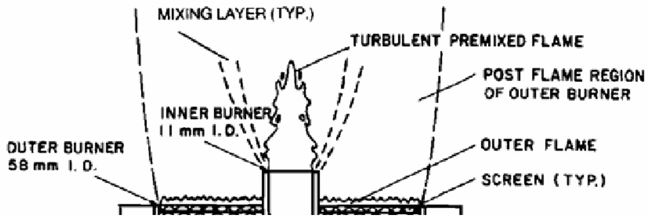

Figure. 1. Bunsen burner setup; adapted from Wu et al. [14].

IV. LES Results and Discussion

Mesh convergence of the LES predictions for the premixed hydrogen Bunsen flames were assessed for the different equivalence ratios by considering the convergence of the total resolved TKE as a function of mesh resolution. For each case, three different meshes were considered: (i) a coarse mesh with around 0.5 million cells; (ii) a medium resolution mesh with 1.0 million cells; and (iii) a fine mesh with 2.0 million cells for the Re $= 40,000$ cases and 1.5 million cells for the Re $= 20,000$ cases. Comparisons of the time evolution of the predicted TKE (not shown here for compactness) with increasing mesh resolution for each of the flames shows a systematic increase in the resolved TKE and an associated decrease in SFS TKE such the total TKE is incrementally increasing and converging to a single quasi-steady value.

Figure 2 shows schlieren photos of the experimental premixed flames in the top panel, and the PCM-FPI LES predictions obtained for fine mesh simulations frame captured at $t=4$ ms in the lower panel, for the Re$=40,000$ cases at three values of the equivalence ratio: $\phi=1.0$, $\phi=1.8$, and $\phi=3.57$. For each LES result, the flame in the center is represented by iso-surfaces for three values on the normalized progress variable: $c=0.1$, 0.5, and 0.9 and the mixing layer as indicated by the darker layers lying outside of the flame is characterized by highly turbulent zones in the shear layer between the jet and the piloted co-flow. A visual comparison shows that, as expected, there is no difference in the wrinkling for the three LES results while, in the experiment, the flame wrinkling clearly increases towards lean limit. Conversely, even if the contributions of the turbulent fluctuation increases towards the rich limit, the preferential diffusion damps or reduces the flame wrinkling for the $\phi = 3.57$ case. In addition, the observed flame height in the experiments for $\phi=1.0$ case shorter than for the $\phi=1.8$ case. This is due to the instabilities caused by preferential diffusion and a resulting increase in the turbulent burning rate. In the case of the LES solutions this trend is inverted and a shorter flame is predicted for $\phi=1.8$ compared to the $\phi=1.0$ case. The reason for this is that the laminar flame speed, S_L, for hydrogen peaks near $\phi=1.8$.

Figure 3 depicts the the complement of the time averaged combustion progress variable, $1 - \bar{c}$ (also called mean unreactedness, with 1 representing fresh mixture) as a function of the axial position along the flame for the Re$=40,000$ cases and compares the experimental values, to the LES predictions. For the sake of completeness, the theory reported by Wu *et al.* [14] is also shown. Results are shown for four values of the equivalence ratio, $\phi=0.8$, $\phi=1.0$, $\phi=1.8$, and $\phi=3.57$ with the darker color representing a higher resolution mesh. Decreasing the LES cell size reduces the numerical dissipation and produces shorter flames the values of which approach the experimental values for unstable conditions corresponding $\phi = 0.8$ and $\phi = 1.0$. For the latter, the PCM-FPI LES predictions agree quite well with the experimental values, but for the former the height is somewhat under-predicted and slope of combustion progress is under-estimated. This is expected, due to the fact that the simulation is not expected to capture the preferential and thermal diffusive phenomena. For $\phi = 1.8$, the highest mixture reactivity is achieved and, as mentioned above, this yields the shortest flame for the LES results. However, due to the destabilizing effects, the most reactive mixture among the experiments is actually the stoichiometric composition and the $\phi= 0.8$ and $\phi=1.0$ exhibit similar flame heights for these reasons. For the last case at $\phi = 3.57$, where diffusion acts as stabilizer, the simulation completely under-predicts the flame height. Figure 4 shows the analogous set of results for the lower Reynolds number Re $= 20,000$ premixed flames. A quick comparison to the Re$=40,000$ cases shows a higher spread in the results for the lower turbulence towards the lean limit where the preferential diffusion effects at lower Reynolds number leads to a more consistent error. This is expected as the turbulence has a relative smaller contribution to the flame wrinkling with lower levels of turbulence. Conversely, the rich mixture simulation exhibit better agreement for the Re$=20,000$ cases because the more turbulence generated wrinkling is damped by stabilizing

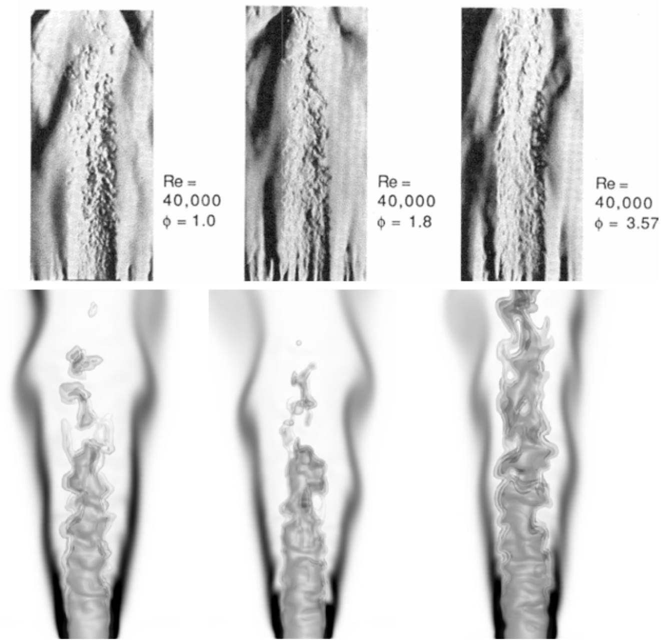

Figure. 2. Comparison between experiment (top) and simulation (bottom) for the Re$=40,000$ turbulent premixed hydrogen-air flames for $\phi=1.0$, $\phi=1.8$, and $\phi = 3.57$. Iso-surfaces of the progress variable are plotted on a slice, darker for higher TKE: the former aims to show the reader the wrinkling of the cases, the latter shows the shear layer generated by the velocity difference of jet and co-flow, and that the flame is not affected by the mixing layer.

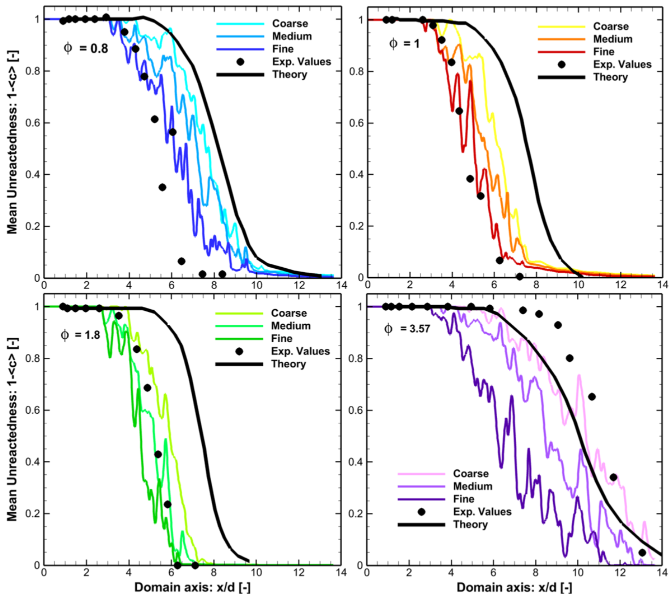

Figure. 3. Mean unreactedness $(1-\overline{c})$: comparison between experiments and simulation. Case: $\mathrm{Re}=40,000$.

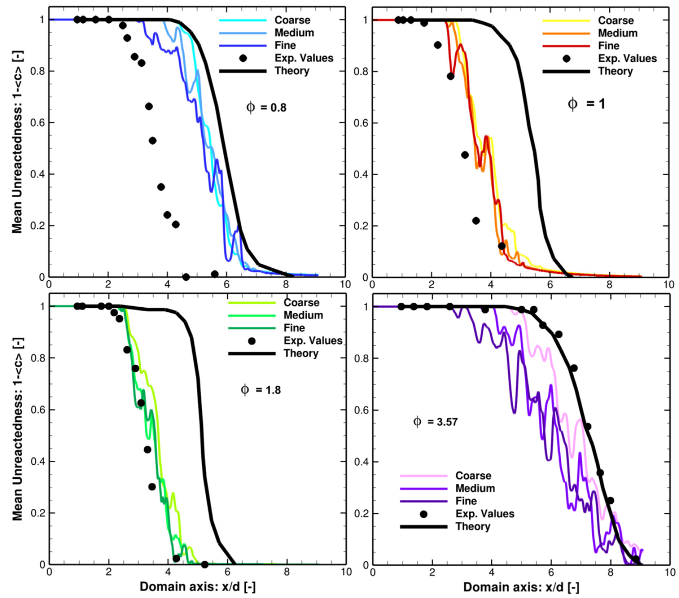

Figure. 4. Mean unreactedness $(1-\overline{c})$: comparison between experiments and simulation. Case: $\mathrm{Re}=20,000$.

effects of the preferential/thermal diffusive mechanisms.

Finally, Fig. 5 provides a direct comparison of the measured flame heights - black curve - and current LES predictions - blue curve, with the red curve depicting the error in the predictions compared to experiment, all as a function of equivalence ratio. Below these curves, the coloured bands indicate the stable and unstable regions for both preferential diffusion and thermal diffusive effects. By first considering the rich limit results with $\phi = 3.57$ and the $\mathrm{Re} = 40,000$ flame, it is very evident how the stabilization effects of these two diffusive phenomena result in an overall burner rate in the actual experiments that is considerably lower than that of LES predictions. As reminder, the LES applied herein does not account for these diffusive effects. As a consequence, the simulated flame height is barely half that of the experimental value. For the same equivalence ratio, but with lower levels of turbulence (i.e., for $\mathrm{Re}=20,000$), the experimental flame height is again underpredicted by the LES; however, to a lesser extent due to the lower levels of turbulence. Somewhat opposite behaviour is observed in the lean limit with $\phi = 0.8$. The enhanced burning rates in the experiments compared to the LES results, due to the effects of preferential diffusion and thermal-diffusive instabilities, which are not modelled in the simulation, are clearly indicated by lower values in the experimental flame heights. Nevertheless, for the higher turbulence case, the predicted flame height of the LES at $\phi = 0.8$ is rather close to the experimental value, due to relative importance of the turbulence and diffusive instabilities on flame wrinkling. For lower turbulence levels (i.e., for $\mathrm{Re}=20,000$), the relative contribution to the flame wrinkling by the diffusive instabilities is higher and the overprediction in the flame height is therefore more evident. Lastly, the range of equivalence ratios associated with a reduction in the slope of the red curve of Fig. 5 depicting the error in the LES flame height provides an indication of the region in which diffusive-thermal stabilization effects compete with preferential diffusion instabilities. For this range of equivalence ratios approaching neutral stability, i.e., $1 < \phi < 1.8$-2, the predicted flame heights of the LES are in very good agreement with the measured values.

V. Conclusions and Future Research

The application of LES to the prediction of turbulent premixed hydrogen flames using the flamelet-based PCM-FPI model has been considered. In particular, PCM-FPI LES predictions of Bunsen-type hydrogen flames with equivalent ratios ranging from $0.8 \leq \phi \leq 3.57$ and for Reynolds numbers of $\mathrm{Re} = 20,000$ and 40,000 were examined and compared to available experimental data with the goal of assessing and quantifying LES errors associated with the treatment (or lack there of) of diffusion effects. The comparisons illustrate well the mutual influence of turbulence and preferential diffusion effects on the turbulent flame structure, burning rate, and flame height. In the lean limit ($\phi = 0.8$) with unstable diffusion conditions, overprediction of flame height and underprediction of turbulent burning rate are observed; however, the relative contributions of both diffusive mechanisms on flame wrinkling are mitigated with increasing turbulence intensity, leading to reductions in these errors. In the rich limit with $\phi=3.57$, the stabilizing effects of preferential diffusion dominate, although now less so for decreasing turbulence levels, and the flame height and burning rates are underpredicted and overpredicted, respectively. Finally, for $\phi=1$ and $\phi=1.8$ (i.e., near neutrally stable flames), the PCM-FPI LES approach quite accurately reproduces the features of the premixed flames, including both flame height and burning rates. Future follow-on research will explore modifications to the PCM-FPI combustion model to account for the effects of both preferential diffusion and diffusive-thermal instabilities in premixed hydrogen flames.

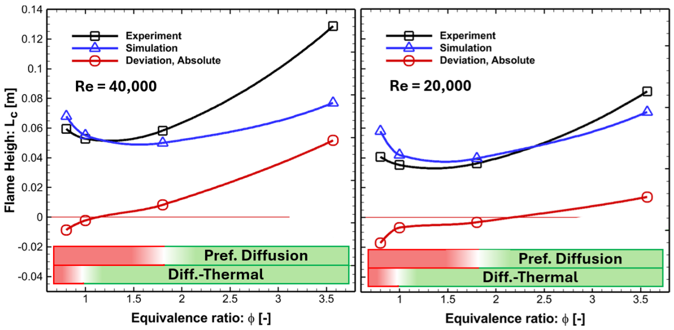

Figure. 5. Comparison of measured and predicted flame heights as a function of fuel equivalence ratio, ϕ, for the $\mathrm{Re}=40,000$ and $\mathrm{Re}=20,000$ turbulent premixed flames. The unstable and stable regimes for preferential diffusion and thermal-diffusive phenomena are also shown.

Acknowledgments

Computational resources were provided by the SciNet High Performance Computing Consortium at the University of Toronto and the Digital Research Alliance of Canada through funding from the Canada Foundation for Innovation (CFI) and the Province of Ontario, Canada.

References

[1] T. S. Ledley, E. T. Sundquist, S. E. Schwartz, D. K. Hall, J. D. Fellows, and T. L. Killeen. Climate change and greenhouse gases. *Eos, Transactions American Geophysical Union*, 80(39):453–458, 1999.

[2] D. W. Kweku, O. Bismark, M. Addae, D. A. Koomson, D. K. Benjamin, E. A. Oti-Mensah, A. T. Quachie, and A. B. Beryl. Greenhouse effect: Greenhouse gases and their impact on global warming. *Journal of Scientific Research and Reports*, 17(6):1–9, 2018.

[3] B. Böhm, J. Brübach, C. Ertem, and A. Dreizler. Experiments for combustion-LES validation. *Flow Turb. Combust.*, 80:507–529, 2008.

[4] R. Cabra, T. Myhrvold, J. Chen, R. Dibble, A. Karpetis, and R. Barlow. Simultaneous laser raman-rayleigh-lif measurements and numerical modeling results of a lifted turbulent H_2/N_2 jet flame in a vitiated coflow. *Proc. Combust. Inst.*, 29(2):1881–1888, 2002.

[5] T. Cheng, J. Wehrmeyer, and R. Pitz. Simultaneous temperature and multispecies measurement in a lifted hydrogen diffusion flame. *Combust. Flame*, 91(3-4):323–339, 1992.

[6] Y. Mizobuchi, S. Tachibana, J. Shinio, S. Ogawa, and T. Takeno. A numerical analysis of the structure of a turbulent hydrogen jet lifted flame. *Proc. Combust. Inst.*, 29(2):2009–2015, 2002.

[7] V. Molkov and J. Saffers. Hydrogen jet flames. *Int. J. Hydrogen Energy*, 38:8141–8158, 2013.

[8] K. Aung, M. Hassan, and G. M. Faeth. Flame stretch interactions of laminar premixed hydrogen/air flames at normal temperature and pressure. *Combust. Flame*, 109(1):1–24, 1997.

[9] K. T. Aung, M. I. Hassan, S. Kwon, L. K. Tseng, O. C. Kwon, and G. M. Faeth. Flame/stretch interactions in laminar and turbulent premixed flames. *Combust. Sci. Tech.*, 174(1):61–99, 2002.

[10] O. Park, P. S. Veloo, H. Burbano, and F. N. Egolfopoulos. Studies of premixed and non-premixed hydrogen flames. *Combust. Flame*, 162(4):1078–1094, 2015.

[11] Y. Chen and R. W. Bilger. Experimental investigation of three-dimensional flame-front structure in premixed turbulent combustion-I: hydrocarbon/air bunsen flames. *Combust. Flame*, 131(4):400–435, 2002.

[12] Y. Chen and R. W. Bilger. Experimental investigation of three-dimensional flame-front structure in premixed turbulent combustion-II: lean hydrogen/air bunsen flames. *Combust. Flame*, 138(1):155–174, 2004.

[14] M. Wu, S. Kwon, J. F. Driscoll, and G. M. Faeth. Turbulent premixed hydrogen/air flames at high reynolds numbers. *Combust. Sci. Tech.*, 73(1-3):327–350, 1990.

[13] Y. Chen and R. W. Bilger. Simultaneous 2-D imaging measurements of reaction progress variable and OH radical concentration in turbulent premixed flames: Experimental methods and flame brush structure. *Combust. Sci. Tech.*, 167(1):131–167, 2001.

[15] M. Wu, S. Kwon, J. F. Driscoll, and G. M. Faeth. Preferential diffusion effects on the surface structure of turbulent premixed hydrogen/air flames. *Combust. Sci. Tech.*, 78(1-3):69–96, 1991.

[16] *Micro Mixing Fuel Injectors for Low Emissions Hydrogen Combustion*, volume Volume 3: Combustion, Fuels and Emissions, Parts A and B of *Turbo Expo: Power for Land, Sea, and Air*, 06 2008.

[17] H. Wang, K. Luo, S. Lu, and J. Fan. Direct numerical simulation and analysis of a hydrogen/air swirling premixed flame in a micro combustor. *Int. J. Hydrogen Energy*, 36(21):13838–13849, 2011. 2010 Asian/APEC BioH2.

[18] *Experimental 3D Analysis of Flame Propagation in a Lean-Premixed Swirl Burner Operated With Hydrogen*, volume Volume 3A: Combustion, Fuels, and Emissions of *Turbo Expo: Power for Land, Sea, and Air*, 06 2023.

[19] M. Tanahashi, M. Fujimura, and T. Miyauchi. Coherent fine-scale eddies in turbulent premixed flames. *Proc. Combust. Inst.*, 28(1):529–535, 2000.

[20] R. Kai, T. Tokuoka, J. Nagao, A. L. Pillai, and R. Kurose. LES flamelet modeling of hydrogen combustion considering preferential diffusion effect. *Int. J. Hydrogen Energy*, 48:11086–11101, 2023.

[21] T. Shoji, Y. Iwasaki, K. Kodai, S. Yoshida, S. Tachibana, and T. Yokomori. Effects of flame behaviors on combustion noise from lean-premixed hydrogen low-swirl flames. *AIAA Journal*, 58(10), October 2020.

[22] G. E. Gioele Ferrante and I. Langella. Differential diffusion modelling for LES of premixed and partially premixed flames with presumed FDF. *Combustion Theory and Modelling*, 28(6):695–730, 2024.

[23] J. Gaucherand, C. Schulze-Netzer, D. Laera, and T. Poinsot. A subgrid-scale model to account for thermo-diffusive effects in artificially thickened LES models for lean turbulent premixed ammonia/hydrogen flames. *Proc. Combust. Inst.*, 40(1):105198, 2024.

[24] Hong G. Im and Jacqueline H. Chen. Preferential diffusion effects on the burning rate of interacting turbulent premixed hydrogen-air flames. *Combustion and Flame*, 131(3):246–258, 2002.

[25] O. Gicquel, N. Darabiha, and D. Thévenin. Laminar premixed hydrogen/air counterflow flame simulations using Flame Prolongation of ILDM with differential diffusion. *Proc. Combust. Inst.*, 28:1901–1908, 2000.

[26] P. Domingo, L. Vervisch, S. Payet, and R. Hauguel. DNS of a premixed turbulent V flame and LES of a ducted flame using a FSD-PDF subgrid scale closure with FPI-tabulated chemistry. *Combust. Flame*, 143:566–586, 2005.

[27] J. Galpin, A. Naudin, L. Vervisch, C. Angelberger, O. Colin, and P. Domingo. Large-eddy simulation of a fuel-lean premixed turbulent swirl-burner. *Combust. Flame*, 155:247–266, 2008.

[28] F. E. Hernández-Pérez, F. T. C. Yuen, C. P. T. Groth, and Ö. L. Gülder. LES of a laboratory-scale turbulent premixed Bunsen flame using FSD, PCM-FPI and thickened flame models. *Proc. Combust. Inst.*, 33:1365–1371, 2011.

[29] F. E. Hernández-Pérez, C. P. T. Groth, and Ö. L. Gülder. Large-eddy simulation of lean hydrogen-methane turbulent premixed flames in the methane-dominated regime. *Int. J. Hydrogen Energy*, 39:7147–7157, 2014.

[30] F. E. Hernández-Pérez. *Subfilter Scale Modelling for Large Eddy Simulation of Lean Hydrogen-Enriched Turbulent Premixed Combustion*. PhD thesis, University of Toronto, April 2011.

[31] N. Shahbazian, M. M. Salehi, C. P. T. Groth, Ö. L. Gülder, and W. K. Bushe. Performance of conditional source-term estimation model for LES of turbulent premixed flames in thin reaction zones regime. *Proc. Combust. Inst.*, 35:1367–1375, 2015.

[32] D. Haworth and T. Poinsot. Numerical simulations of lewis number effects in turbulent premixed flames. *J. Fluid Mech.*, 244:405–436, 1992.

[33] R. S. Rogallo. Numerical experiments in homogeneous turbulence. Technical Memorandum 81315, NASA, September 1981.

[34] P. Roe. Approximate riemann solvers, parameter vectors, and difference schemes. *J. Fluid Mech.*, 43(2):357–372, 1981.